Conductance and valley splitting in etched Si/SiGe one-dimensional nanostructures

G. Frucci, L. Di Gaspare, and F. Evangelisti
Dipartimento di Fisica, Università Roma TRE, Via Vasca Navale 84, 00146 Roma, Italy

E. Giovine and A. Notargiacomo
Istituto di Fotonica e Nanotecnologie-CNR, Via Cineto Romano 42, 00156 Roma, Italy

V. Piazza and F. Beltram
NEST, Scuola Normale Superiore and Istituto Nanoscienze-CNR, Piazza San Silvestro 12, 56127 Pisa, Italy
(Received 19 February 2010; revised manuscript received 19 April 2010; published 10 May 2010)

The conductance of strongly confined one-dimensional constrictions fabricated from Si/SiGe two-dimensional electron gases is investigated. Conductance measurements reveal conductance quantization in units of $G_0=2e^2/h$ rather than $2G_0=4e^2/h$, as expected in the presence of valley and spin degeneracy. Furthermore, at temperatures below $T=400$ mK, small steps and peaklike features, superimposed to the conductance plateaus, become visible. The conductance in the presence of parallel and perpendicular magnetic field shows that significant valley splitting is present even at zero magnetic field. The enhanced valley splitting observed in our etched devices is related to the strong in-plane confinement.

DOI: 10.1103/PhysRevB.81.195311 PACS number(s): 73.23.Ad, 73.21.Hb

I. INTRODUCTION

Investigation of electronic transport in low-dimensional SiGe systems is presently a subject of increasing interest, motivated not only by the obvious relevance of silicon as the most important electronic material but also by recent suggestions that Si/SiGe heterostructures may be very promising for the realization of solid-state qubits exhibiting long coherence time.[1] In fact, thanks to the small spin-orbit coupling and the predominance of spin-zero nuclear isotopes, long intrinsic spin-coherence times are expected. However, a crucial drawback for the implementation of quantum computing in this material is represented by the sixfold valley degeneracy of cubic-Si conduction-band minima. Indeed, multiple minima can open additional paths for decoherence which can, in principle, decrease spin lifetime.[2] In a Si/SiGe-based two-dimensional electron gas (2DEG), the in-plane tensile strain present in the Si channel reduces the conduction-band degeneracy, which becomes twofold for the lowest minimum.[3] As a consequence, in one-dimensional (1D) channels based on tensile Si, quantum transport is expected to take place through spin- and valley-degenerate 1D subbands and to exhibit a conductance quantum of $2G_0=4e^2/h$ in the framework of the independent-electron picture for carrier transport. Indeed, $4e^2/h$ quantization was reported in early investigations.[4–6] This twofold valley degeneracy can however be lifted in heterostructures by the sharp confining potential at quantum-well interfaces. The latter couples the two-valley states and results in a valley splitting predicted to be in the 0.1–1 meV range for both Si/SiGe and Si/SiO_2 heterostructures.[7–9]

The valley-splitting magnitude is an oscillating function of well thickness, a behavior that originates from intervalley reflection of the electron wave off the quantum-well interfaces.[10–12] A straightforward consequence of this property is that thickness fluctuations or steps at real interfaces can change valley splitting.[2] Interference effects and thereby valley-splitting oscillations can be partially suppressed by the presence of electrical field in the growth direction, as in the case of modulation-doped heterostructures, due to the squeezing of the electronic wave function to one side of the quantum well.[8,10]

Advanced theoretical models for the study of transport properties in 2D interacting systems underlined that transport in multivalley electron gas can be strongly affected by intervalley scattering rate.[13,14] In Ref. 13, it was shown that when valley-splitting energy and inverse of intervalley scattering rate have comparable values both parameters are necessary to describe experimental conductivity data.

From an experimental point of view, many papers reported valley-splitting values smaller than the predicted ones.[2,15–18] An exception is the large valley splitting recently reported for a Si/SiO_2 quantum well,[19] a result that to date was not understood theoretically. Conductance quantization in multiples of $G_0=2e^2/h$ was found in nanosize vertical silicon structures.[20] In this paper, authors speculated that the narrow size of the conducting channel could be responsible for the removal of valley degeneracy, leading to the observed $2e^2/h$ steps. More recently, Goswami *et al.*[2] showed that valley splitting can be controlled and improved by combining electrostatic and magnetic confinement in nanostructures since confinement can enhance valley splitting by reducing the number of steps explored by electronic wave functions.

In order to investigate the possible enhancement of valley splitting by a strong in-plane confining potential, in the present work we investigate quantum conductance in narrow channels fabricated by etching. Our data show that large valley splitting can indeed be obtained, depending on the fabrication process. However, conductance spectra are also affected by transmission resonances due to electron backscattering induced by the nonadiabatic confining potential and, possibly, defects.

II. EXPERIMENTAL

We fabricated two kinds of 1D devices, whose schematics and scanning electron microscopy (SEM) images are shown

 ©2010 The American Physical Society

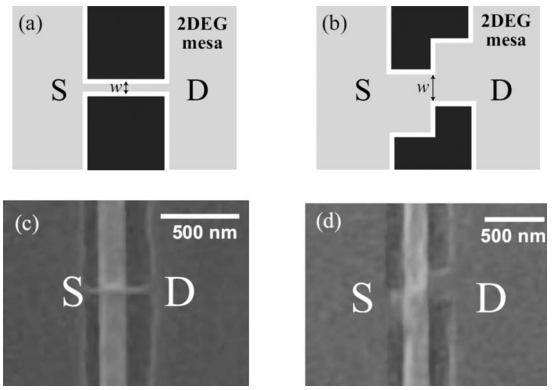

FIG. 1. (a) and (b) Top-view schematics of the mesa defining the wire and the QPC prior to gate deposition. S and D indicate source and drain contacts in the 2DEG, respectively, w is the geometrical width of the 1D channel; (c) and (d) SEM images of two actual devices with metallic gates (vertical stripes).

in Fig. 1. Devices were fabricated by combining electron-beam lithography and reactive ion etching starting from Si/SiGe samples containing 2DEGs. As shown in Figs. 1(a) and 1(c), in one kind of device (referred to as *wire* in the following), the 1D constriction was obtained by crossing a 40-nm-wide and 450-nm-long wire with a Ti/Au 180-nm-wide gate so that the carrier density could be modulated. S and D in the figure indicate the wide 2DEG portions acting as source and drain contacts. The second kind of device is shown in Figs. 1(b) and 1(d) and will be referred to as *quantum point contact* (QPC). In this case, the 1D constriction results from the narrow channel originating at the corner of the two square-shaped protrusions. A 150-nm-wide gate crossing the constriction allows the modulation of the carrier density.

The starting 2DEGs were obtained in Si/SiGe modulation-doped heterostructures, grown by ultrahigh-vacuum chemical-vapor deposition on Si(001) substrates. Details of the layer sequence thickness as well as the structural and morphological properties of deposited heterostructures are described elsewhere.[21] The mobility and carrier density of the 2DEGs were determined through low-field Hall measurements on mesa etched Hall bars. The wire shown in panel (c) was fabricated on a 2DEG with mobility and carrier density equal to $\mu=1.5\times10^4$ cm^2 V^{-1} s^{-1} and $n=9.4\times10^{11}$ cm^{-2} at 15 K, corresponding to a mean-free path $l\approx340$ nm. As for the QPC reported in panel (d), it was obtained from a 2DEG with mobility, carrier density, and mean-free path at 15 K equal to $\mu=1.0\times10^4$ cm^2 V^{-1} s^{-1}, $n=9.2\times10^{11}$ cm^{-2}, and $l\approx225$ nm, respectively. In both devices, the estimated mean-free path on the order of hundreds of nanometers ensures that charge propagation in the region of interest occurs in the quasiballistic regime.

Linear- and nonlinear-conductance ($G=dI/dV_{SD}$) behavior was investigated as a function of gate bias, magnetic field, and temperature. The measurements were performed in a ^{3}He refrigerator with a base temperature of 0.26 K by using low-frequency (17 Hz) lock-in techniques. Great care was paid to decrease the electromagnetic interference that can affect low-level signals.

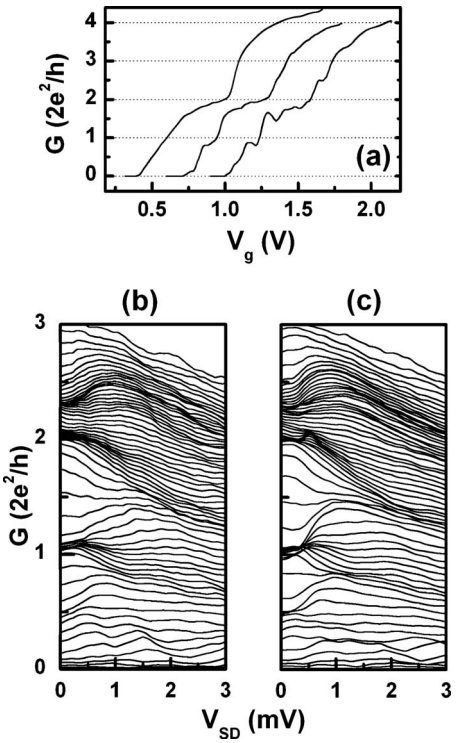

FIG. 2. Linear and nonlinear conductance of the wire acquired at different temperatures: (a) linear-conductance curves reported for decreasing temperatures: from left to right, $T=4.1$ K, $T=2.0$ K, and $T=0.26$ K, respectively. Curves are horizontally offset by 0.3 V for clarity; (b) and (c) nonlinear-conductance curves $G(V_{SD})$ as a function of the positive source-drain bias V_{SD} for gate voltage varying in the 0.3–1.05 V range acquired at 1.5 K and 0.3 K, respectively.

III. RESULTS AND DISCUSSION

The linear conductance as a function of gate bias of the wire device shown in Fig. 1(c) is reported in Fig. 2(a) at three different temperatures. At $T=4.1$ K, two rounded plateaus only are present in the G trace, at $G=2G_0$ and $G=4G_0$, i.e., at the quantization values expected for valley and spin degeneracy. Upon lowering the temperature at $T=2.0$ K, an additional plateau at $G=G_0$ becomes clearly visible. For $T=0.4$ K and below, small steps and peaklike features develop and superimpose to the plateaus. As we shall show in the following, the $G=G_0$ plateau results from the presence of an appreciable valley splitting while the superimposed fine structure originates from multiple reflections due to transmission resonances caused by the nonadiabatic 1D-2D transition of the potential at the ends of the 1D channel and/or by scattering at defects.

Figures 2(b) and 2(c) show the nonlinear conductance measured as a function of V_{SD} in the 0.3–1.05 V V_g range at a temperature of 1.5 K and 0.3 K, respectively. Coherently with a conductance quantization in units of G_0, transport data exhibit an accumulation of traces at multiples of G_0 around zero bias. In addition, the peaklike features superimposed to the conductance plateaus give rise to trace accumulation at noncanonical G values such as $0.5G_0$ and $2.3G_0$. For finite V_{SD}, curves tend to merge at half integers of the conductance

quantum G_0, as expected when the number of conducting subbands for the two transport directions differs by one.[22] Thus, linear and nonlinear transport data in the narrow etched wire confirm the occurrence of conductance plateau-like structures at G_0 and $2G_0$, and indicate that transport is taking place through twofold-degenerate transverse modes.

A more detailed investigation of steps and peaklike features appearing for G in the $0G_0-2G_0$ range was performed in the etched QPC devices. Note that below the $2G_0$ quantum value, no structures should be present in case of ideal spin and valley degeneracy. Figure 3(a) shows linear-conductance curves taken as a function of V_g at $T=0.26$ K. Reported curves are acquired in several gate-voltage sweeps performed at constant temperature by varying gate voltage from pinch-off toward positive values. Total acquisition time for each G trace was about 30 min. Figure 3(b) reports linear-conductance curves taken at different temperatures. Inspection of the curves in panel (a) shows that the main steplike and peaklike features are quite reproducible but fine details and absolute conductance values slightly change from sweep to sweep. The reproducibility in different cooldowns can be surmised from the comparison of spectra in Fig. 3(a) with the right curve of Fig. 3(b) and the $H=0$ curve of Fig. 4(a) which were recorded in different refrigeration cycles. The main characteristics of the linear conductance versus V_g can be summarized as follows. At $G=G_0$, a marked feature is always present, whose line shape alternates between steplike and peaklike. At lower G values, a prominent steplike feature is present at $G\sim 0.6G_0$ in Fig. 3(a), which assumes a peaklike line shape in Figs. 3(b) and 4(a) at $G\sim 0.8$ and $G\sim 0.85G_0$, respectively. Figure 3(b) shows that features exhibited by the curves at different measuring temperatures are quite "robust" since at $T=1.6$ K they are still visible.

The presence of the peaklike features in the linear-conductance curves is accompanied by the appearance of zero-bias anomalies in the nonlinear conductance [see Fig. 3(c) where the nonlinear $G=dI/dV_{SD}$ curves at 0.38 K as a function of the source-drain voltage V_{SD} are reported for V_g values in the −0.04–1.04 V range]. At V_{SD} near zero, a fine structure is present whose line shape varies strongly upon changing V_g. A comparison between linear- and nonlinear-conductance curves reveals that this zero-bias fine structure appears in the $G(V_{SD})$ curves for V_g values corresponding to the two prominent peaklike features present in the linear G traces in Fig. 3(a).

The presence of additional structures in the G curves, missing plateaus, the presence of zero-bias anomalies and in general deviations from experimental-conductance "canonical" quantized values were reported also in the GaAs systems.[23–27] Some effects appear to be intrinsic to mesoscopic devices, e.g., the additional plateau below G_0 (the so-called 0.7 anomaly[25]). Other features were related to extrinsic mechanisms such as an asymmetric distribution of the electron density on the two sides of the QPC (Ref. 27) or scattering events.[28] Indeed, scattering or partial reflection of electron waves can produce both transmission resonances and reduced conductance values and can be caused by defects or irregularity in the potential or reflection at both ends of the conducting channel.

In summary, the conductance measurements in our etched devices exhibit features in the $0G_0-2G_0$ range that can have

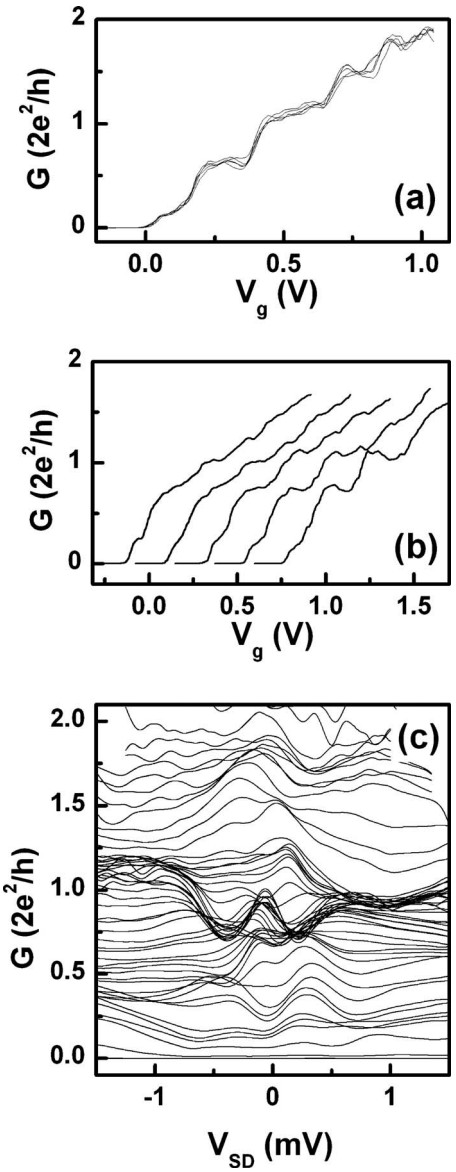

FIG. 3. Linear and nonlinear conductance of the QPC acquired at different temperatures: (a) several linear-conductance curves as a function of gate voltage taken at $T=0.26$ K in the same cooldown are reported in order to appreciate the range of their variability; (b) linear-conductance curves acquired at $T=1.6$ K, 1.4 K, 0.9 K, 0.6 K, and 0.38 K, from left to right, respectively. Traces are horizontally offset by 0.225 V for clarity; (c) nonlinear-conductance curves $G(V_{SD})$ taken at a fixed gate voltage in the −0.04–1.04 V range at $T=0.38$ K.

different origins, the more likely being a partial removal of the conduction-band degeneracy due to valley splitting and resonances due to geometrical and/or impurity backscattering. Magnetotransport measurements were used to discriminate among the different possibilities. In particular, if the additional features were due to carrier scattering, restoring of conductance quantization and a flattening of conductance plateaus would be expected by applying perpendicular magnetic fields.[28] On the other hand, since a parallel magnetic field acts on the electron spin only without affecting orbital motion, at high fields the presence of spin degeneracy should

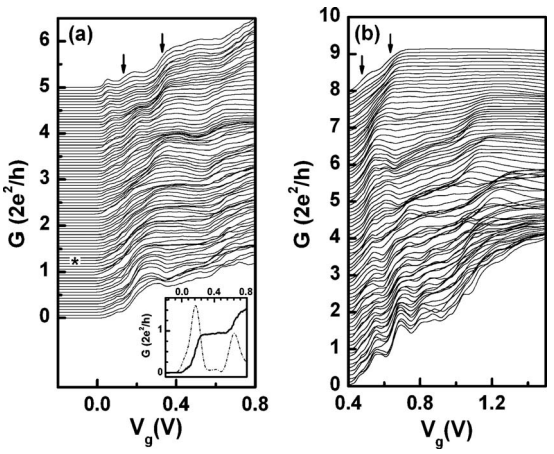

FIG. 4. Linear conductance versus gate voltage in a perpendicular magnetic field. (a) QPC: the data, taken at $T=0.38$ K, are shown from $H=0$ T (bottom curve) to $H=8$ T (top curve), in steps of 0.1 T and vertically offset by $0.125G_0$ for clarity; inset: conductance curve taken at 1.2 T [bold line, curve marked with the asterisk in panel (a)] and its numerical derivative (dashed-dotted line). (b) Wire: the data, taken at $T=0.26$ K, are shown from $H=0$ T (bottom curve) to $H=8$ T (top curve). The curves are vertically offset by $0.1G_0$ for clarity.

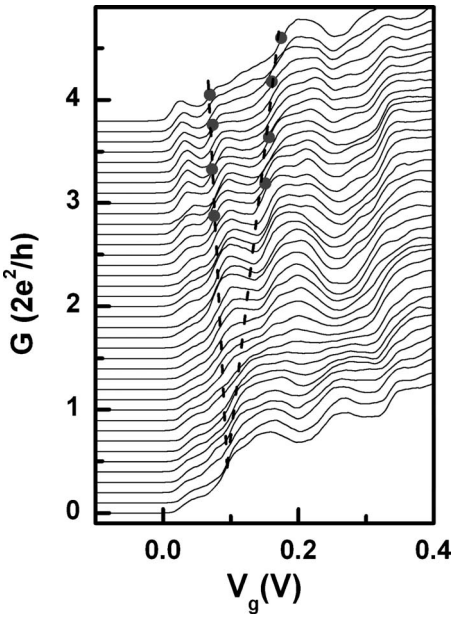

FIG. 5. Evolution of the conductance versus V_g for the QPC in a parallel magnetic field ranging from $H=0$ T (bottom curve) to $H=7.6$ T (top curve) in steps of 0.2 T. The curves are taken at $T=0.38$ K and vertically offset by $0.1G_0$ for clarity. Dots indicate the edges corresponding to the Zeeman-split 1D mode and dashed lines are the linear fits of the edge V_g positions as a function of the magnetic field.

manifest through the appearance of conductance plateaus at half G_0 due to Zeeman splitting.

Linear-conductance data as a function of the gate voltage in perpendicular magnetic field are reported in Fig. 4. The data pertaining to the QPC are shown in Fig. 4(a). Upon increasing magnetic field intensity, we observe both a flattening of the peaklike feature at $G=0.85G_0$ and a concomitant rising of its conductance with a well-developed flat plateau occurring at $G=G_0$ for magnetic fields larger than 1.1 T (see the inset where the G trace at $B=1.2$ T is shown). Both these findings are distinctive signatures of the magnetic suppression of the electron interference due to backscattering trajectories[28] and point to resonances of backscattered electrons as the origin of the peaklike features present for $T<0.4$ K. We note that the flat $G=G_0$ plateau is restored at a magnetic field value for which the electron cyclotron diameter is comparable to the size of the 200-nm-wide square-shaped 2DEG protrusions in Fig. 1(d). This observation suggests that the magnetic field suppresses the interference of the geometrical backscattering paths caused by the boundaries of the etched protrusions.

The behavior of the linear conductance of the wire sample in the presence of a perpendicular magnetic field is reported in Fig. 4(b). Analogously to the behavior observed with the QPC, it is evident that the plateaus become flatter and more pronounced with increasing H, a behavior once again interpreted as a magnetic suppression of the interference of geometrical backscattering paths. In this narrow-wire device, however, the suppression of the geometrical backscattering occurs at higher fields since the wire width is smaller. Figure 4(b) suggests that backscattering at the constriction is completely inhibited for magnetic fields larger than 6 T, when a wide and flat $G=G_0$ plateau develops. Indeed, at $H=6$ T the cyclotron diameter is equal to 53 nm, consistently with the wire width. For H larger than 7 T, a single and wide $G=G_0$ plateau is present in the G curves. It can also be noted from a general overview of the conductance behavior that at fixed gate voltages, the conductance decreases as the magnetic field increases, the signature of magnetic depopulation of hybrid subbands.[29]

In summary, magnetotransport measurements on the two devices allow us to unambiguously distinguish the intrinsic features present in the linear-conductance curves from the extrinsic ones caused by geometrical backscattering and point out the presence in both devices of a $G=G_0$ plateau that we attribute to the removal of the twofold valley degeneracy in the conduction band of the tensile Si channel.

In order to evaluate the magnitude of this valley splitting, we determined the factor converting gate-bias V_g values to electron energies in the 1D constriction by exploiting conductance measurements under parallel magnetic field. The conductance evolution of the QPC in parallel magnetic field is reported in Fig. 5. Despite the presence of features due to backscattering that are insensitive to parallel magnetic field, it is evident that at large fields, the first feature splits into two prominent plateaulike structures at $0.5G_0$ and $1G_0$. The corresponding V_g values shift almost linearly as a function of the magnetic field as expected for the Zeeman effect. We interpret this evolution as the removal of the remaining spin degeneracy in the $G=G_0$ plateau. The V_g edge positions (dots in Fig. 5) of the $0.5G_0$ and $1G_0$ structures were determined from the maxima of the numerical first derivative of the G curves. From the linear fit of the measured V_g separations as a function of magnetic field and assuming $g=2$ for Si (Ref. 2), we obtained a conversion factor η between electron energy and gate voltage of 4.3 ± 0.4 meV V^{-1}.

We note that at high-field values, spin splitting is also detectable for perpendicular magnetic fields. Indeed, in the case of the QPC upon increasing magnetic field intensity, the conductance spectra exhibit a splitting into two prominent plateaulike structures [arrows in the top curve of Fig. 4(a)] again at $0.5G_0$ and $1G_0$ values whose behavior is very similar to that observed in the presence of a parallel magnetic field, as expected for the Zeeman removal of spin degeneracy. The estimated η value is equal to that determined from the analysis of parallel magnetic field measurements.

For the wire sample, conductance curves taken for intense perpendicular magnetic fields exhibit a split of the $G=1G_0$ that we interpret again as a signature of the Zeeman spin splitting [arrows in the top curve of Fig. 4(b)]. The conversion factor was determined to be $\eta=7.7\pm0.8$ meV V^{-1}.

We finally evaluated the valley-splitting energy for the wire from the V_g separation of the $G=1G_0$ and $G=2G_0$ plateaus of the intermediate curve in Fig. 2(a). We obtained a zero-field valley-splitting energy of 1.1 ± 0.1 meV. Unfortunately, for the QPC, the persistence of peaklike features due to backscattering makes this procedure not applicable at zero magnetic field. A more reliable determination can be made in the case of perpendicular magnetic fields that suppress backscattering so that a well-developed plateau is present in the spectra. As shown for the curve at 1.2 T in the inset of Fig. 4(a), we could estimate the valley-splitting energy from the V_g separation of the $G=1G_0$ and $G=2G_0$ conductance edges and found for the QPC a valley splitting equal to 2.0 ± 0.2 meV. Note, however, that this value may have been somewhat increased by the widening of the plateaus due to magnetic depopulation in 1D constriction[29] or valley-splitting dependence on magnetic field strength.[2,30]

In the case of quantum wells with perfectly flat (100) interfaces, a theoretical valley splitting on the order of 1 meV is predicted.[10] Several authors reported measured valley-splitting energies smaller than the predicted ones.[15,16] One possible explanation for the discrepancy between theoretical predictions and experimental findings is discussed in Ref. 2. These authors argue that the atomic steps present at quantum-well interfaces and the consequent thickness fluctuations are responsible for the valley-splitting suppression compared to the case of ideal flat interfaces. Indeed, theoretical valley-splitting values oscillate as a function of well width and, therefore, if the electron wave function extends over a region where steps are present valley splitting may average to a smaller mean value. By the same reasoning, lateral confinement can enhance the valley splitting by decreasing the number of steps probed by the wave function. In agreement with this scheme, recently Goswami *et al.*[2] reported valley-splitting enhancement up to 1.5 meV due to electrostatic and magnetic confinement in a Si QPC.

As for our devices, they were fabricated by using a hybrid approach in which confinement generated by physical etching of the 2DEG is combined with a Schottky gate for the electrostatic control of the carrier density in the constriction. First we note that a built-in electrical field is present in our samples along the growth direction due to both asymmetric growth sequence of the modulation-doped 2DEG and gate bias. The presence of an electrical field (both built-in and induced by gate bias) weakens the dependence of valley-splitting magnitude on well thickness, as theoretical works predicted.[8,10] In the limit of strong field, the valley splitting does not depend on the well width and its magnitude is expected to be on the order of a millielectron volt.[8] We believe that this effect together with the strong lateral confinement peculiar of these devices do play a dominant role in determining the observed valley splitting. Indeed, confinement by physical reduction of the region in which electrons are present can be an efficient method to limit valley-splitting averaging. Thickness fluctuations can be particularly significant in this respect owing to the intrinsic roughness stemming from strain in Si/SiGe heterostructures.

IV. CONCLUSIONS

The independent-electron picture for carrier transport predicts a conductance quantization in multiple integers of $2G_0=4e^2/h$ due to spin and valley degeneracy in Si/SiGe-based 1D devices. On the contrary, in our etched devices, linear- and nonlinear-conductance analysis indicates that conductance is quantized in $1G_0$ units. We ascribed this observations to the removal of valley degeneracy. The analysis of the conductance behavior in perpendicular and parallel magnetic fields confirmed this interpretation and allowed us to quantitatively evaluate valley-splitting magnitude.

[1] B. E. Kane, Nature (London) **393**, 133 (1998).
[2] S. Goswami, K. A. Slinker, M. Friesen, L. M. McGuire, J. L. Truitt, C. Tahan, L. J. Klein, J. O. Chu, P. M. Mooney, D. W. van der Weide, R. Joynt, S. N. Coppersmith, and M. A. Eriksson, Nat. Phys. **3**, 41 (2007).
[3] F. Schäffler, Semicond. Sci. Technol. **12**, 1515 (1997).
[4] S. L. Wang, P. C. van Son, B. J. van Wees, and T. M. Klapwijk, Phys. Rev. B **46**, 12873 (1992).
[5] D. Többen, D. A. Wharam, G. Abstreiter, J. P. Kotthaus, and F. Schäffler, Semicond. Sci. Technol. **10**, 711 (1995).
[6] U. Wieser, U. Kunze, K. Ismail, and J. O. Chu, Appl. Phys. Lett. **81**, 1726 (2002).
[7] L. J. Sham and M. Nakayama, Phys. Rev. B **20**, 734 (1979).
[8] M. Friesen, S. Chutia, C. Tahan, and S. N. Coppersmith, Phys. Rev. B **75**, 115318 (2007).
[9] C. Tahan, M. Friesen, and R. Joynt, Phys. Rev. B **66**, 035314 (2002).
[10] T. B. Boykin, G. Klimeck, M. A. Eriksson, M. Friesen, S. N. Coppersmith, P. von Allmen, F. Oyafuso, and S. Lee, Appl. Phys. Lett. **84**, 115 (2004).
[11] T. B. Boykin, G. Klimeck, M. Friesen, S. N. Coppersmith, P. von Allmen, F. Oyafuso, and S. Lee, Phys. Rev. B **70**, 165325 (2004).
[12] M. O. Nestoklon, E. L. Ivchenko, J.-M. Jancu, and P. Voisin,

Phys. Rev. B **77**, 155328 (2008).
[13] N. N. Klimov, D. A. Knyazev, O. E. Omel'yanovskii, V. M. Pudalov, H. Kojima, and M. E. Gershenson, Phys. Rev. B **78**, 195308 (2008).
[14] A. Punnoose and A. M. Finkel'stein, Phys. Rev. Lett. **88**, 016802 (2001).
[15] P. Weitz, R. J. Haug, K. von. Klitzing, and F. Schaffler, Surf. Sci. **361-362**, 542 (1996).
[16] S. J. Koester, K. Ismail, and J. O. Chu, Semicond. Sci. Technol. **12**, 384 (1997).
[17] M. A. Wilde, M. Rhode, Ch. Heyn, D. Heitmann, D. Grundler, U. Zeitler, F. Schaffler, and R. J. Haug, Phys. Rev. B **72**, 165429 (2005).
[18] K. Lai, T. M. Lu, W. Pan, D. C. Tsui, S. Lyon, J. Liu, Y. H. Xie, M. Muhlberger, and F. Schäffler, Phys. Rev. B **73**, 161301(R) (2006).
[19] K. Takashina, Y. Ono, A. Fujiwara, Y. Takahashi, and Y. Hirayama, Phys. Rev. Lett. **96**, 236801 (2006).
[20] K. Nishiguchi and S. Oda, Appl. Phys. Lett. **76**, 2922 (2000).
[21] L. Di Gaspare, K. Alfaramawi, F. Evangelisti, E. Palange, G. Barucca, and G. Majni, Appl. Phys. Lett. **79**, 2031 (2001).
[22] N. K. Patel, J. T. Nicholls, L. Martin-Moreno, M. Pepper, J. E. F. Frost, D. A. Ritchie, and G. A. C. Jones, Phys. Rev. B **44**, 13549 (1991).
[23] A. Yacoby, H. L. Stormer, Ned S. Wingreen, L. N. Pfeiffer, K. W. Baldwin, and K. W. West, Phys. Rev. Lett. **77**, 4612 (1996).
[24] D. Kaufman, Y. Berk, B. Dwir, A. Rudra, A. Palevski, and E. Kapon, Phys. Rev. B **59**, R10433 (1999).
[25] K. J. Thomas, J. T. Nicholls, M. Y. Simmons, M. Pepper, D. R. Mace, and D. A. Ritchie, Phys. Rev. Lett. **77**, 135 (1996).
[26] C.-T. Liang, M. Y. Simmons, C. G. Smith, D. A. Ritchie, and M. Pepper, Appl. Phys. Lett. **75**, 2975 (1999).
[27] A. Shailos, A. Ashok, J. P. Bird, R. Akis, D. K. Ferry, S. M. Goodnick, M. P. Lilly, J. L. Reno, and J. A. Simmons, J. Phys.: Condens. Matter **18**, 1715 (2006).
[28] B. J. van Wees, L. P. Kouwenhoven, E. M. M. Willems, C. J. P. M. Harmans, J. E. Mooij, H. van Houten, C. W. J. Beenakker, J. G. Williamson, and C. T. Foxon, Phys. Rev. B **43**, 12431 (1991).
[29] B. J. van Wees, L. P. Kouwenhoven, H. van Houten, C. W. J. Beenakker, J. E. Mooij, C. T. Foxon, and J. J. Harris, Phys. Rev. B **38**, 3625 (1988).
[30] S. Lee and P. von Allmen, Phys. Rev. B **74**, 245302 (2006), and references therein.